International Journal of Mechanical, Industrial and Aerospace Sciences
ISSN: 2517-9950
Vol:7, No:11, 2013

Geometrically Non-Linear Axisymmetric Free Vibration Analysis of Functionally Graded Annular Plates

Boutahar Lhoucine, El Bikri Khalid, Benamar Rhali

Abstract**—**In this paper, the non-linear free axisymmetric vibration of a thin annular plate made of functionally graded material (FGM) has been studied by using the energy method and a multimode approach. FGM properties vary continuously as well as non-homogeneity through the thickness direction of the plate. The theoretical model is based on the classical plate theory and the Von Kármán geometrical non-linearity assumptions. An approximation has been adopted in the present work consisting of neglecting the in-plane deformation in the formulation. Hamilton's principle is used to derive the governing equation of motion. The problem is solved by a numerical iterative procedure in order to obtain more accurate results for vibration amplitudes up to 1.5 times the plate thickness. The numerical results are given for the first axisymmetric non-linear mode shape for a wide range of vibration amplitudes and they are presented either in tabular form or in graphical form to show the effect that the vibration amplitude and the variation in material properties have significant effects on the frequencies and the bending stresses in large amplitude vibration of the functionally graded annular plate.

Keywords**—**Non-linear vibrations. Annular plates. Large amplitudes. FGM.

I. Introduction

FUNCTIONALLY graded materials (FGMs) are the new microscopic inhomogeneous composite materials. These Materials are usually made of a combination of ceramic and metal such that the material properties vary smoothly and continuously in appropriate direction(s). The continuity in the material properties of these new materials provides better mechanical behavior in comparison with the fiber-reinforced composites. A combination of the properties of the metal and ceramic can be achieved by the composition of them. These properties that consist of high-temperature resistance due to low thermal conductivity, wear and oxidation resistance for ceramics and the high toughness, high strength, mach inability and bonding capability for metals, cause that FGMs can resist high-temperature conditions while their toughness maintains.

Because of these good characteristics, FGMs have extensively used in various industries such as space structures, turbo machinery, nuclear and chemical industries, defense mechanisms, energy conversion systems.

Due to this widespread applicability, FGMs have been extensively studied by researchers in recent years, particularly the vibration analyses of functionally graded structures like as plates are carried out by many researchers.

For example, Reddy and Cheng [5] studied the harmonic vibration problem of functionally graded plates by means of a three-dimensional asymptotic theory formulated in terms of transfer matrix. Allahverdizadeh and Naei [3] studied nonlinear free and forced vibration analysis of thin circular functionally graded plates and investigated the amplitude and thermal effects on the nonlinear behavior of those plates. They also studied the effects of large vibration amplitudes on the stresses of thin circular functionally graded plates. Chen [4] analyzed the nonlinear vibration of a shear deformable functionally graded plate by using the equations that include the effects of transverse shear deformable and rotary inertia. Amini et al. [1] studied stress analysis for thick annular functionally graded plate. They used first order shear deformation plate and von Kármán type equation.

Their results revealed that vibration amplitude and volume fraction have significant effect on resultant stresses in large amplitude vibration of functionally graded thick plate.

The aim of this paper is to study nonlinear free vibration of thin annular functionally graded plates. Material properties are assumed to be graded in the thickness direction according to a simple power law distribution in terms of the volume fractions of the constituents. The formulations are based on Classic Plate Theory and von Kármán-type equation.

In the present work, axisymmetric free large vibration amplitudes of thin functionally graded annular plates are investigated by using and adapting the model applied successfully to geometrically non-linear free and forced vibrations of various structures such as simply supported and clamped–clamped beams, homogeneous and composite rectangular plates, and shells [6], [7], [9], [12]. By supposing harmonic motion and expanding the transverse displacement in the form of finite series of basic functions, the linear free vibration modes of an annular plate have both edges clamped, obtained in terms of Bessel's functions, the discretized expressions for the total strain energy and kinetic energy have been derived. Hamilton's principle is used to reduce the large amplitude free vibration problem to a set of non-linear algebraic equations, which have been solved by a numerical iterative procedure.

Numerical results are presented in both dimensionless tabular and graphical forms, and highlight the influence of material composition on induced bending stress in large amplitude vibration of thin annular functionally graded plates.

Boutahar Lhoucine and El Bikri Khalid are with the Université Mohammed V-Souissi ENSET- rabat, LaMIPI, B.P6207, Rabat Instituts, Rabat, Morocco (e-mail: lhoucine.boutahar@um5s.net.ma, k.elbikri@um5s.net.ma).

Benamar Rhali is with the Université Mohammed V-Agdal, EMI. LERSIM, Agdal Av.Ibn Sina, Rabat, Morocco (e-mail: rbenamar@emi.ac.ma).

II. General Formulation

A. Problem Definition

Consider a functionally annular plate of thin uniform thickness $h = 0.01$ with outer radius $a = 0.5$, inner radius $b = 0.05$, as depicted in Fig. 1. The annular plate geometry and dimensions are defined in the cylindrical coordinates (r, θ, z). The FGM plate material is made of a combination of ceramic and metal. The top surface $(z = h/2)$ of the plate is ceramic-rich whereas the bottom surface $(z = -h/2)$ is metal-rich.

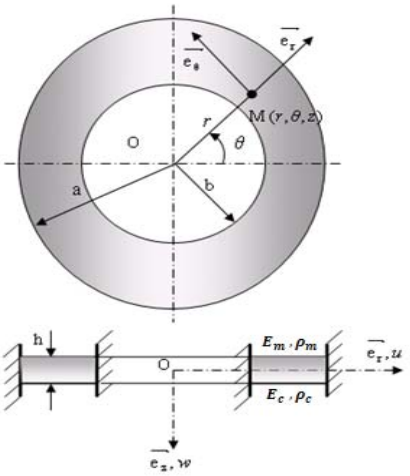

Fig. 1 Annular plate geometry, dimensions and notation

In the case of large amplitude axisymmetric vibrations of the annular plate, the radial displacement u_r and the transverse displacement u_z show the displacement of the point with $M(r, z)$ coordinate. By using the Kirchhoff plate theory, u_r and u_z are expressed as:

$$u_r(r, z, t) = u(r, t) - z\,\partial w(r, t)/(\partial r) \tag{1}$$

$$u_z(r, t) = w(r, t) \tag{2}$$

where $u(r, t)$ and $w(r, t)$ are the radial and transverse displacements of the point on the middle surface of the plate respectively, and t is the time variable.

On the basis of geometric non-linear theory of thin plates in von Karman's sense, one obtains the strain-displacement relations:

$$\varepsilon_r = (\partial u/\partial r) + (1/2)(\partial w/\partial r)^2 - z\,(\partial^2 w/\partial r^2) \tag{3}$$

$$\varepsilon_\theta = (u/r) - \left(\frac{z}{r}\right)(\partial w/\partial r) \tag{4}$$

where ε_r and ε_θ are the radial and tangential strains, respectively.

B. Total Strain and Kinetic Energies Expressions

By using Hooke's law, the radial and circumferential stresses are given by:

$$\sigma_r = \frac{E(z)}{(1-\upsilon^2)}(\varepsilon_r + \upsilon\varepsilon_\theta) \tag{5}$$

$$\sigma_\theta = \frac{E(z)}{(1-\upsilon^2)}(\varepsilon_\theta + \upsilon\varepsilon_r) \tag{6}$$

The total strain energy is expressed as:

$$V = \frac{1}{2}\iiint \sigma_{ij}\,\varepsilon_{ij} dv\ , dv = r dr d\theta\, dz \tag{7}$$

which can be written as:

$$V = \frac{1}{2}\int_b^a \int_0^{2\pi} \int_{-h/2}^{h/2} (\sigma_r \varepsilon_r + \sigma_\theta \varepsilon_\theta) r dr d\theta\, dz \tag{8}$$

or like the sum of the strain energy due to bending V_b and the membrane strain energy induced by large deflections V_m

$$V = V_b + V_m \tag{9}$$

The bending strain energy is given by:

$$\begin{aligned} V_b = -\pi B_{11} \int_b^a & [(\partial w/\partial r)^2 (\partial^2 w/\partial r^2)] r dr \\ & - \pi B_{12} \int_b^a [(1/r)\,(\partial w/\partial r)(\partial w/\partial r)^2] r dr \\ & + \pi D_{11} \int_b^a [(\partial^2 w/\partial r^2)^2 + (1/r^2)\,(\partial w/\partial r)^2]\, r dr \\ & + 2\,\pi D_{12} \int_b^a [(1/r)(\partial w/\partial r)(\partial^2 w/\partial r^2)]\ r dr \end{aligned} \tag{10}$$

By neglecting the axial motion, the membrane strain energy induced by large deflections of the annular plate can be written as:

$$\mathrm{V_m} = (\pi \mathrm{A_{11}}/4) \int_\mathrm{b}^\mathrm{a} (\partial \mathrm{w}/\partial \mathrm{r})^4 \mathrm{r dr} \tag{11}$$

where A_{11}, B_{11} and D_{11} are the extension-extension, bending-extension, bending-bending coupling coefficients respectively, and can be evaluated as follows,

$$(A_{11}, B_{11}, D_{11}) = \int_{-h/2}^{h/2} \frac{E(z)}{1-\vartheta^2}\ (1, z, z^2)\ dz \tag{12}$$

$$B_{12} = \upsilon B_{11}\ , D_{12} = \upsilon D_{11} \tag{13}$$

By neglecting the rotary inertia, the kinetic energy of the annular plate can be written as:

$$T = \frac{1}{2}\int \left(\frac{\partial w}{\partial t}\right)^2 dm\ , dm = \rho(z) r d\theta dr dz \tag{14}$$

$$T = \frac{1}{2}\int_{-h/2}^{h/2} \rho(z) dz \int_0^{2\pi} d\theta \int_b^a \left(\frac{\partial w}{\partial t}\right)^2 r dr \tag{15}$$

$$T = \pi I_0 \int_b^a \left(\frac{\partial w}{\partial t}\right)^2 rdr \quad (16)$$

where

$$I_0 = \int_{-h/2}^{h/2} \rho(z)\, dz \quad (17)$$

C. Discretization of the Total and Kinetic Energies Expressions

The transverse displacement function is expanded as a series of space functions and the time function. These functions are supposed to be separable, and the transverse displacement can be written as:

$$w(r,t) = w(r).q(t) \quad (18)$$

The space function $w(r)$ is expanded in the form of finite series of n basic functions $w_i(r)$ as:

$$w(r). = a_i w_i(r) \quad (19)$$

If harmonic motion is assumed the time function can be written as:

$$q(t) = sin(\omega t) \quad (20)$$

By using the summation convention for repeated indices over the range $([1,\dots,n]$, the expression for transverse displacement is then given by:

$$w(r,t) = a_i w_i(r) sin(\omega t) \quad (21)$$

Substituting the expression given in (21) into (10), (11) and (16), one obtains:

$$V_m = (1/2)(\pi A_{11}/2) a_i a_j a_k a_l sin^4(\omega t) \int_b^a (\partial w_i/\partial r)(\partial w_j/\partial r)(\partial w_k/\partial r)(\partial w_l/\partial r) rdr \quad (22)$$

$$V_m = (1/2) a_i a_j a_k a_l (\pi A_{11}/2) b_{ijkl} sin^4(\omega t) \quad (23)$$

where b_{ijkl} is the non-linearity tensor, given by:

$$b_{ijkl} = \int_b^a (\partial w_i/\partial r)(\partial w_j/\partial r)(\partial w_k/\partial r)(\partial w_l/\partial r) rdr \quad (24)$$

$$\begin{aligned} V_b &= \frac{1}{2} 2\pi D_{11} a_i a_j sin^2(\omega t) \int_b^a (\partial^2 w_i/\partial r^2)(\partial^2 w_j/\partial r^2)\, rdr \\ &+ \frac{1}{2} 2\pi D_{11} a_i a_j sin^2(\omega t) \int_b^a (1/r^2)\,(\partial w_i/\partial r)(\partial w_j/\partial r) rdr \\ &- \frac{1}{2} 2\pi B_{11} a_i a_j a_k sin^2(\omega t) \int_b^a (\partial^2 w_i/\partial r^2)(\partial w_i/\partial r)(\partial w_i/\partial r)\, rdr \\ &- \frac{1}{2} 2\pi B_{11} a_i a_j a_k sin^2(\omega t) \int_b^a (\upsilon/r)\,(\partial w_i/\partial r)(\partial w_j/\partial r)(\partial w_i/\partial r)\, rdr \end{aligned} \quad (25)$$

$$V_b = \frac{1}{2} a_i a_j 2\pi D_{11} k_{ij} sin^2(\omega t) + \frac{1}{2} a_i a_j a_k 2\pi B_{11} c_{ijk} sin^3(\omega t) \quad (26)$$

$$V = \frac{1}{2} a_i a_j 2\pi D_{11} k_{ij} sin^2(\omega t) + \frac{1}{2} a_i a_j a_k 2\pi B_{11} c_{ijk} sin^3(\omega t) + \frac{1}{2} a_i a_j a_k a_l (\pi A_{11}/2) b_{ijkl} sin^4(\omega t) \quad (27)$$

where k_{ij} and c_{ijk} are the rigidity tensor and the coupling tensor, respectively, and given by:

$$k_{ij} = \int_b^a (\partial^2 w_i/\partial r^2)(\partial^2 w_j/\partial r^2)\, rdr + \int_b^a 1/r^2\, (\partial w_i/\partial r)(\partial w_j/\partial r) rdr \quad (28)$$

$$c_{ijk} = -\int_b^a (\partial^2 w_i/\partial r^2)(\partial w_i/\partial r)(\partial w_i/\partial r)\, rdr \int_b^a (\upsilon/r)\,(\partial w_i/\partial r)(\partial w_j/\partial r)(\partial w_i/\partial r)\, rdr \quad (29)$$

$$T = \tfrac{1}{2} 2\pi I_0\, \omega^2 a_i a_j cos^2(\omega t) \int_b^a w_i w_j\, rdr \quad (30)$$

$$T = \frac{1}{2} \omega^2 a_i a_j 2\pi I_0 m_{ij} cos^2(\omega t) \quad (31)$$

where m_{ij} is the mass tensor, given by:

$$m_{ij} = \int_b^a w_i w_j\, rdr \quad (32)$$

D. Governing Equations

A Hamilton's principle applied in the present work for study the dynamic behavior of the plate, is symbolically written as:

$$\partial \int_0^{2\pi/\omega} (V - T) dt = 0 \quad (33)$$

In which ∂ indicates the variation of the integral.

Introducing the (27) and (31) into the energy condition (33) via reduces the problem to that of finding the minimum of the function φ given by:

$$\begin{aligned} \varphi = \frac{1}{2} a_i a_j 2\pi D_{11} k_{ij} \int_0^{2\pi/\omega} sin^2(\omega t)\, dt + \frac{1}{2} a_i a_j a_k a_l (\pi A_{11}/2) b_{ijkl} \int_0^{2\pi/\omega} sin^4(\omega t)\, dt \\ + \frac{1}{2} a_i a_j a_k 2\pi B_{11} c_{ijk} \int_0^{2\pi/\omega} sin^3(\omega t)\, dt \\ - \frac{1}{2} \omega^2 a_i a_j 2\pi I_0 m_{ij} \int_0^{2\pi/\omega} cos^2(\omega t)\, dt \end{aligned} \quad (34)$$

With respect to the undetermined constant a_i.Integrating the trigonometric functions $\sin^2(\omega t), \sin^3(\omega t), \sin^4(\omega t)$ and $\cos^2(\omega t)$ over the range [0, 2π/ω] leads to the following expression:

$$\varphi = (\pi / 4\omega) a_i a_j k_{ij} + (3\pi / 16\omega)\, \zeta\, a_i a_j a_k a_l b_{ijkl} + (2\beta / 3\omega) a_i a_j a_k c_{ijk} - (\pi\gamma / 2\omega) a_i a_j\, m_{ij} \quad (35)$$

where,

$$\zeta = (A_{11}/4\, D_{11}), \beta = (-B_{11}/D_{11}), \gamma = (I_0/D_{11}) \quad (36)$$

In this expression, φ appears as a function of only the undetermined constant a_i. $i = 1, \ldots, n$

Equation (33) reduces to:

$$\partial\varphi/\partial a_r = 0\,,\ r = 1, \ldots, n \tag{37}$$

Generally, the tensors m_{ij} and k_{ij} are symmetric, the tensors b_{ijkl} and c_{ijk} are such that:

$$b_{ijkl} = b_{kjij}\ ;\ b_{ijkl} = b_{jilk} \tag{38}$$

$$c^s_{ijk} = (1/3)\big(c_{ijk} + c_{ijk} + c_{ijk}\big) \tag{39}$$

Taking into account these properties of symmetry, it appears that (37) are equivalent to the following set of nonlinear algebraic equations:

$$a_i k_{ir} + \frac{3}{2}\zeta a_i a_j a_k b_{ijkr} + \frac{4}{\pi}\beta a_i a_j c^s_{ijr} - \gamma\omega^2 a_i m_{ir} = 0 \tag{40}$$
$$r = 1, \ldots, n$$

Equation (40) represents a set of n non-linear algebraic equations relating the n coefficients a_i and the frequency ω.

$$\omega^2 = \frac{a_i a_j k_{ij} + (3/2)\zeta a_i a_j a_k a_l b_{ijkl} + (4/\pi)\beta a_i a_j c^s_{ijk}}{\gamma a_i a_j m_{ij}} \tag{41}$$

which has to be substituted in (40) to obtain a system of n non-linear algebraic equations' leading to the n contribution coefficients $a_i\,; i = 1, \ldots, n$.

Adopting the solution procedure used in [1]-[4], the contribution coefficient a_{r0} of the basic function corresponding to the desired mode (the first mode is considered in this paper) r_0 is first fixed, and the other basic function contribution coefficients are calculated via numerical solution of the remaining $(n-1)$ non-linear algebraic equations (40) for $r \neq r_0$

$$a_i k_{ir} + \frac{3}{2}\zeta a_i a_j a_k b_{ijkr} + \frac{4}{\pi}\beta a_i a_j c^s_{ijr} - \gamma\omega^2 a_i m_{ir} = 0 \tag{42}$$

The values obtained for a_i, for $i \neq r_0$, are then substituted into (41) to obtain the corresponding value of ω^2_{r0}.

To obtain non-dimensional parameters, we put:

$$w_i(r) = h w^*_i(r^*);\ \alpha = b/a\,;\ r = a r^*$$

$$m_{ij}/{m_{ij}}^* = a^2 h^2\,;\ \ k_{ij}/{k_{ij}}^* = h^2/a^2 \tag{43}$$

$$b_{ijkl}/{b_{ijkl}}^* = h^4/a^2\,;\ c_{ijk}/{c_{ijk}}^* = h^3/a^2$$

${m_{ij}}^*$, ${k_{ij}}^*$ and ${c_{ijk}}^*$ and ${b_{ijkl}}^*$ are non dimensional tensors given by:

$${m_{ij}}^* = \int_\alpha^1 w^*_i w^*_j r^* dr^* \tag{44}$$

$$k^*_{ij} = \int_\alpha^1 (\partial^2 w^*_i/\partial r^{*2})(\partial^2 w^*_j/\partial r^{*2})\ r^* dr^* + \int_\alpha^1 (1/r^{*2})(\partial w^*_i/\partial r^*)(\partial w^*_j/\partial r^*)\ r^* dr^* \tag{45}$$

$${c_{ijk}}^* = -\int_\alpha^1 (\partial^2 w^*_i/\partial r^{*2})(\partial w^*_j/\partial r^*)(\partial w^*_k/\partial r^*)\, r^* dr^* - \int_\alpha^1 (\upsilon/r)(\partial w^*_i/\partial r^*)(\partial w^*_j/\partial r^*)(\partial w^*_k/\partial r^*)\, r^* dr^* \tag{46}$$

$${b_{ijkl}}^* = \int_\alpha^1 (\partial w^*_i/\partial r^*\, \partial w^*_j/\partial r^*\, \partial w^*_k/\partial r^*\, \partial w^*_l/\partial r^*) r^* dr^* \tag{47}$$

Substituting these equations into (40) and (41) leads to:

$$a_i k^*_{ir} + \frac{3}{2}\zeta a_i a_j a_k b^*_{ijkr} + \frac{4}{\pi}\beta a_i a_j c^{s*}_{ijr} - \gamma\omega^2 a_i m^*_{ir} = 0 \tag{48}$$

$$\omega^{*2} = \frac{a_i a_j k^*_{ij} + (3/2)\zeta a_i a_j a_k a_l b^*_{ijkl} + (4/\pi)\beta a_i a_j c^{s*}_{ijk}}{\gamma a_i a_j m^*_{ij}} \tag{49}$$

The set of non-linear algebraic equations (40) can be written in a matrix form as:

$$[Kl^* + Knl^*]\{A\} - \omega^{*2}[M^*]\{A\} = \{0\} \tag{50}$$

where $[M^*]$; $[Kl^*]$ and $[Knl^*]$ are the non-dimensional mass matrix, the non dimensional linear stiffness matrix and the non-dimensional non-linear geometrical stiffness matrix, respectively. Each term of the matrix $[Knl^*]$ is a quadratic function of the column matrix of coefficient $\{A\} = [a_1, a_2, a_3 \ldots\ldots, a_n]^T$; and is given by:

$$Knl^*_{ij} = (3/2)\zeta a_i a_j a_k a_l b^*_{ijkl} + (4/\pi)\beta a_i a_j c^{s*}_{ijk} \tag{51}$$

It can be seen that when the non-linear term is neglected, the nonlinear eigenvalue problem (50) reduces to the classical eigenvalue problem which is the Rayleigh–Ritz formulation of the linear vibration problem.

$$[Kl^*]\{A\} - \omega^2[M^*]\{A\} = \{0\} \tag{52}$$

In the linear case, the eigenvalue equation (52) leads to a series of eigenvalues and corresponding eigenvectors.

In the non-linear case, the solution of (50) should lead to a set of amplitude-dependent eigenvectors, with their amplitude dependent associated eigenvalues. In the present work, the iterative method of solution is used for to solve the non-linear eigenvalue problem (50).

E. Stress Expressions

The bending strains ε_{br} and $\varepsilon_{b\theta}$ are given by:

$$\varepsilon_{br}(z) = -z(d^2w/dr^2)\,;\varepsilon_{b\theta}(z) = -(z/r)\,(dw/dr) \tag{53}$$

The in-plane membrane strains ε_{mr} and $\varepsilon_{m\theta}$ are given by:

$$\varepsilon_{mr}(z) = (du/dr) + (1/2)(dw/dr)^2, \varepsilon_{m\theta}(z) = u/r \tag{54}$$

By using the classical thin plate assumption of plane stress and Hooke's law, the radial and circumferential bending stresses are given by:

$$\sigma_{br} = -\frac{zE(z)}{(1-\nu^2)}[(d^2w/dr^2) + (\upsilon/r)\,(dw/dr)] \quad (55)$$

$$\sigma_{b\theta} = -\frac{zE(z)}{(1-\nu^2)}[(1/r)(dw/dr) + \upsilon\,(d^2w/dr^2)] \quad (56)$$

and the radial and circumferential membrane stresses are given by:

$$\sigma_{mr} = \frac{E(z)}{(1-\nu^2)}[(du/dr) + (1/2)(dw/dr)^2 + \upsilon(u/r)] \quad (57)$$

$$\sigma_{m\theta} = \frac{E(z)}{(1-\nu^2)}[(u/r) + \upsilon((du/dr) + (1/2)(dw/dr)^2)] \quad (58)$$

By neglecting the in-plane displacement u, the membrane stresses are negligible.

In terms of the non-dimensional parameters defined in the previous section, the radial and circumferential bending stresses σ_{br} and $\sigma_{b\theta}$ can be defined by:

$$\sigma_{br} = -\frac{zE(z)h}{(1-\nu^2)a^2}\left[\frac{d^2w^*}{dr^{*2}} + \frac{\upsilon}{r^*}\frac{dw^*}{dr^*}\right] \quad (59)$$

$$\sigma_{b\theta} = -\frac{zE(z)h}{(1-\nu^2)a^2}\left[\frac{1}{r^*}\frac{dw^*}{dr^*} + \upsilon\frac{d^2w^*}{dr^{*2}}\right] \quad (60)$$

F. Properties of Functionally Graded Material

The material properties P of the FG plate are assumed to vary continuously through the thickness of the plate as a function of the volume fraction $V_i$and the properties of constituent materials P_i. These properties can be determined by the simple rule of mixture as [2]-[11].

$$P = \sum_{i=1}^{n} P_i V_i \qquad P = E\,,\rho\,,\upsilon\,,.. \quad (61)$$

where P_i and V_i are the material properties and volume fraction respectively of the constituent material i and n is number of the constituent material.

TABLE I
MATERIAL PROPERTIES OF METAL AND CERAMIC CONSTITUENTS OF AN ANNULAR FGM PLATE [9]

Materials	E(GPa)	ν
Ceramic (Zirconia)	110.25	0.288
Metal (Aluminum)	278.41	0.288

E: Young's modulus
υ: Poisson's ratio
ρ: Mass density

It is clear that the sum of volume fractions of the constituent materials should be:

$$\sum_{i=1}^{n} V_i = 1 \quad (62)$$

A simple power law distribution [10] is used for the volume fraction of the constituents' material across the thickness of the plate. This is defined as:

$$V_i(\mathrm{z}) = \left(\frac{z}{h} + \frac{1}{2}\right)^N \quad (63)$$

$V_i(\mathrm{z})$ denote the volume fraction of constituent material i ; z is the thickness coordinate $(-h/2 \le z \le h/2)$ and N is the volume fraction index which takes values greater than or equal to zero $(0 \le N \le \infty)$.

Here, the FGM is combined of metal and ceramic $n = 2$ $P = E\,,\rho$. The variation of Poisson's ratio υ is generally small and it is assumed to be a constant for convenience. The detail of this FGM is presented in Table I.

From (61) to (63) one has:

$$P(z) = P_m V_m + P_c V_c \quad (64)$$

$$V_m + V_c = 1 \quad (65)$$

$$V_c(\mathrm{z}) = \left(\frac{z}{h} + \frac{1}{2}\right)^N, V_m(\mathrm{z}) = 1 - \left(\frac{z}{h} + \frac{1}{2}\right)^N \quad (66)$$

$V_c(\mathrm{z})$ and $V_m(\mathrm{z})$ denote the volume fraction of ceramic and metal, respectively.

The value of (N) equal to zero represents the fully metal, and for (N) equal to infinity represents the fully ceramic .For $(\mathrm{N} = 1)$ there is a linear variation of the composition of constituents.

$$E(z) = E_c V_c + E_m V_m \;,\; \rho(z) = \rho_c V_c + \rho_m V_m \quad (67)$$

Introduction of (66) into (64) leads to the material properties of the FGM plate as:

$$E(z) = (E_c - E_m)\left(\frac{z}{h} + \frac{1}{2}\right)^N + E_m \quad (68)$$

$$\rho(z) = (\rho_c - \rho_m)\left(\frac{z}{h} + \frac{1}{2}\right)^N + \rho_m \quad (69)$$

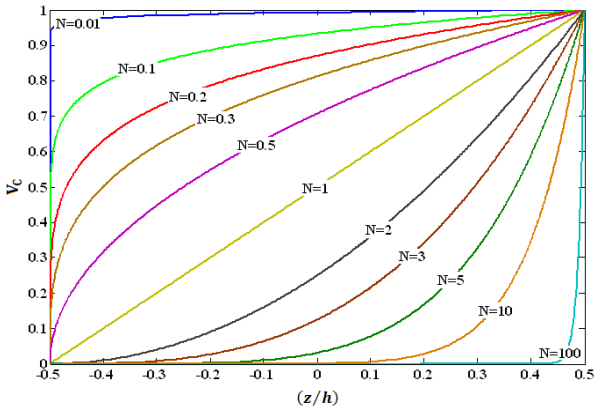

Fig. 2 Variation of ceramic volume fraction through the dimensionless thickness for different values of volume fraction index

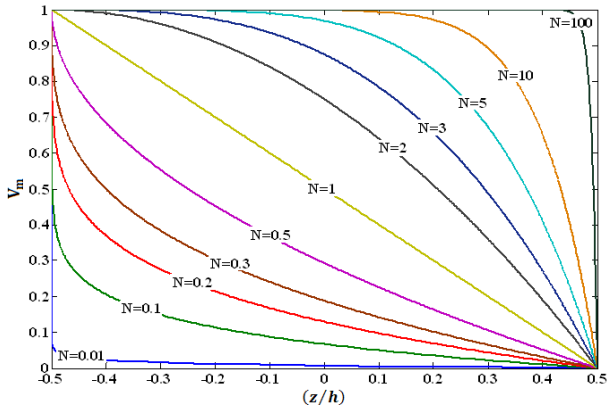

Fig. 3 Variation of metal volume fraction through the dimensionless thickness for different values of volume fraction index

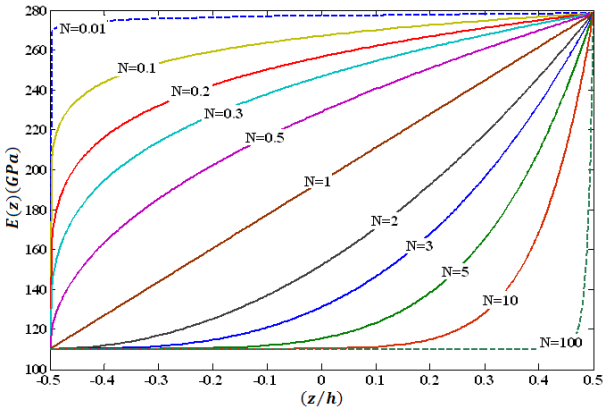

Fig. 4 Variation of Young's modulus of FG plate through the dimensionless thickness for different values of volume fraction index

G. Determination of the Non- Linear Mode Shapes of Thin Isotropic Annular Plate Having Both Edges Clamped

In this work, the Rayleigh method is used to analyze the free vibrations and determine the fundamental linear frequencies. The method is taken from [8]-[13]. Numerical results thus obtained are summarized in Table II with comparing results with those in the literature.

TABLE II
DIMENSIONLESS FREQUENCY PARAMETERS FOR THE ANNULAR PLATE WITH CLAMPED OUTER AND INNER EDGE (C-C) ($\upsilon = 0.3$)

Results	Mode	b/a			
	(m, n)	0.1	0.3	0.5	0.7
Leissa [13]		27.3000	45.2000	89.2000	248.0000
Vera and Febbo[8]	(0, 1)	27.2800	45.3460	89.2500	248.4020
Present study		27.2805	45.3462	89.2508	248.4021
Leissa [13]		28.4000	46.6000	90.2000	249.0000
Vera and Febbo[8]	(1, 1)	28.9150	46.6430	90.2300	249.1640
Present study		28.9158	46.6435	90.2303	249.1639
Leissa [13]		36.7000	51.0000	93.3000	251.0000
Vera and Febbo[8]	(2, 1)	36.6170	51.1380	93.3210	251.4800
Present study		36.6173	51.1388	93.3212	251.4806
Leissa [13]	(3, 1)	51.2000	60.0000	99.0000	256.0000
Present study		51.2188	60.0335	98.9280	255.4438

To obtain the fundamental non-linear mode shapes, the first six axisymmetric linear mode shapes were used. The corresponding non-dimensional linear frequencies $(\Omega_L^*)_i$ $i = 1, \ldots, 6$ are given in Table III and the corresponding curves are plotted in Fig. 5.

TABLE III
NON-DIMENSIONAL LINEAR FREQUENCIES $(\Omega_L^*)_i$; ASSOCIATED WITH THE AXISYMMETRIC LINEAR MODES OF A THIN ANNULAR PLATE HAVING BOTH EDGES CLAMPED $(\alpha = 0.1)$ FOR $i = 1, .., 6$

i	1	2	3	4	5	6
$(\Omega_L^*)_i$	27.280	75.366	148.213	245.484	367.175	513.268

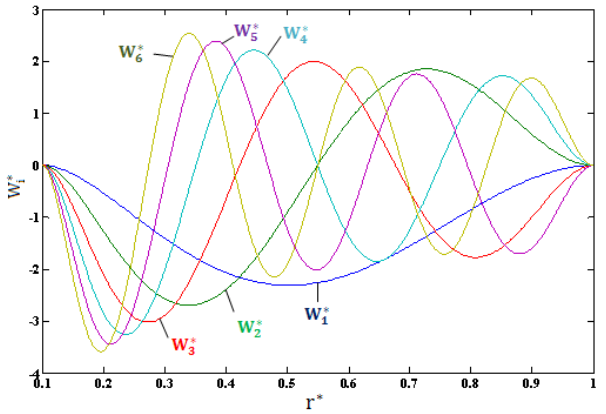

Fig. 5 Non-dimensional axiymmetric linear modes shape w_i^* (r^*) of free vibration for an annular plate having both edges clamped $(\alpha = 0.1)$ for $i = 1, \ldots, 6$

III. Numerical Results and Discussions

In order to determine the results of the present study, the non-linear vibration of an annular FGM plate having both edges has been solved using the iterative method of solution

The first non-linear normalized axisymmetric mode shape for various values of (N) is plotted in Fig. 6. It may be seen that the effect of various values of (N) on this mode shape is negligible.

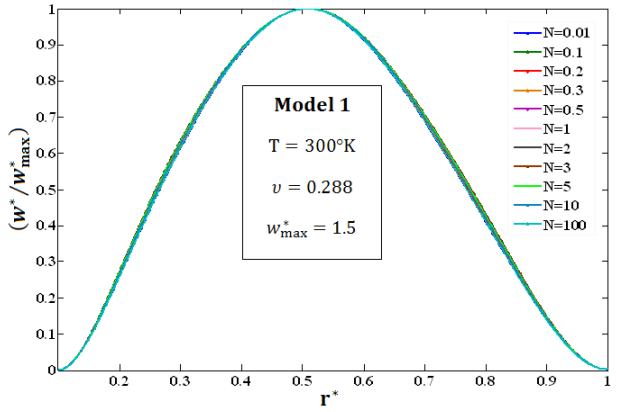

Fig. 6 First non-linear normalized axiymmetric mode shape of free an annular plate having both edges clamped for different values of (N)

The variation of non-dimensional frequency ratio with dimensionless maximum vibration amplitude associated with the first non-linear axisymmetric mode shape of an annular FG plate having both edges clamped for different values of (N) is plotted in Fig. 7.

At a given amplitude the frequencies increase legerment relative to those of an annular isotropic plate (N = 0, N = ∞) for values of (N) varying from 0 to 0.5 and decreases legerment for values of volume fraction index (N) varying from 2 to 10.This variation increases with the amplitude but it remains low.

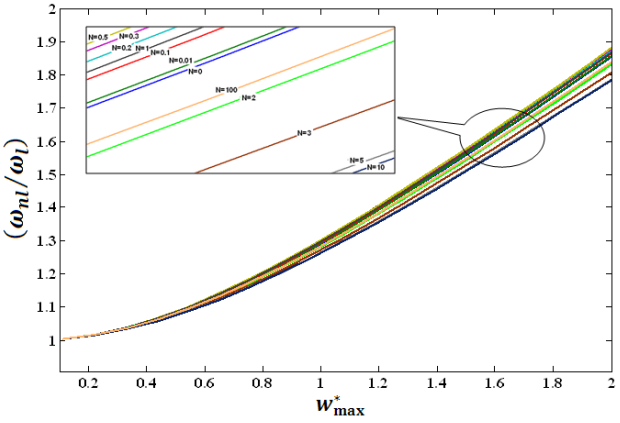

Fig. 7 Variation of non-dimensional frequency ratio with dimensionless maximum vibration amplitude associated with the first non-linear axisymmetric mode shape of an annular FG plate having both edges clamped for different values of (N)

In Figs. 8 and 11 are plotted the variation of the radial and circumferential stresses with dimensionless radius from a surface to another for (N = 0.5) to see the variation of the bending stresses with dimensionless radius from a rich-metal surface to rich-ceramic surface.

In Figs. 9, 10, 12 and 13 are plotted the variation of radial and circumferential stresses with dimensionless maximum vibration amplitude on different surfaces for (N = 0.5) at the inner and outre edges of annular FG plate, for defining the most stressed surface.

From these figures, it is observed that the bending stresses at the geometrical middle surface $(z/h = 0)$ remain unchanged and the most stressed area is rich ceramic surface.

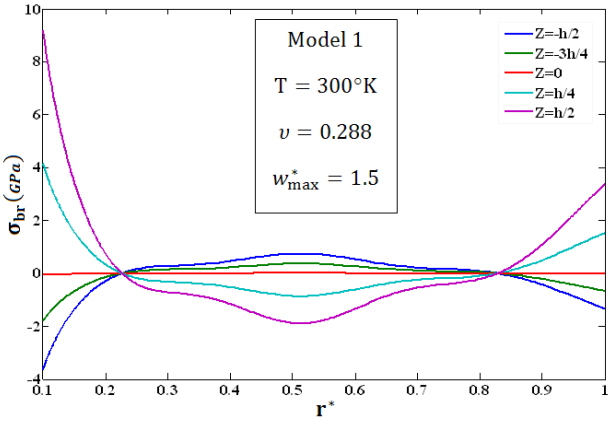

Fig. 8 Variation of radial stress with dimensionless radius on different surfaces for N = 0.5

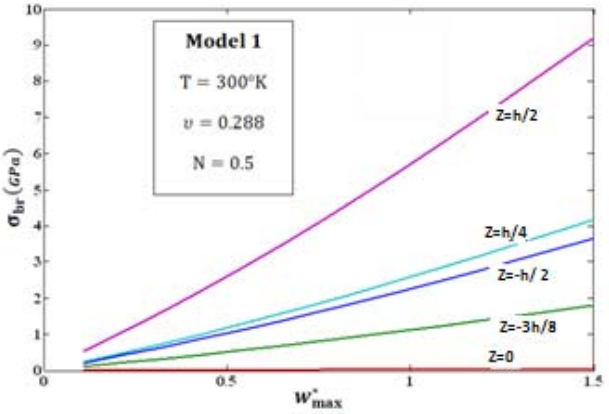

Fig. 9 Variation of radial stress with dimensionless maximum vibration amplitude on different surfaces for N = 0.5 at the inner edge

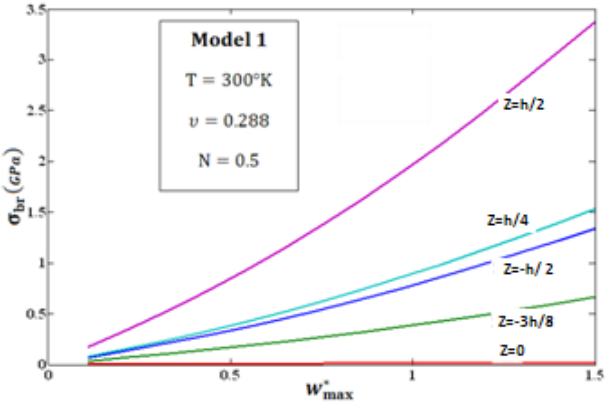

Fig. 10 Variation of radial stress with dimensionless maximum vibration amplitude on different surfaces for N = 0.5 at the outre edge

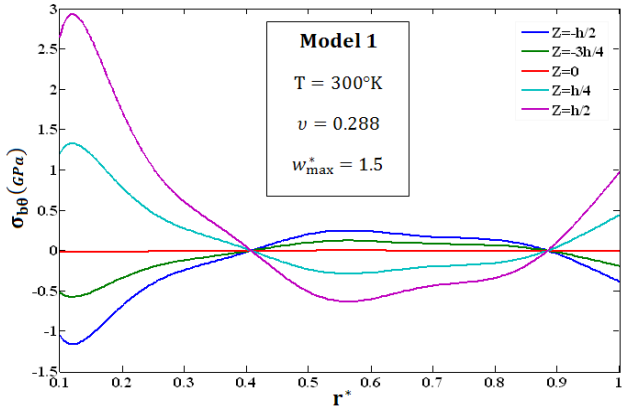

Fig. 11 Variation of circumferential stress with dimensionless radius on different surfaces for N = 0.5

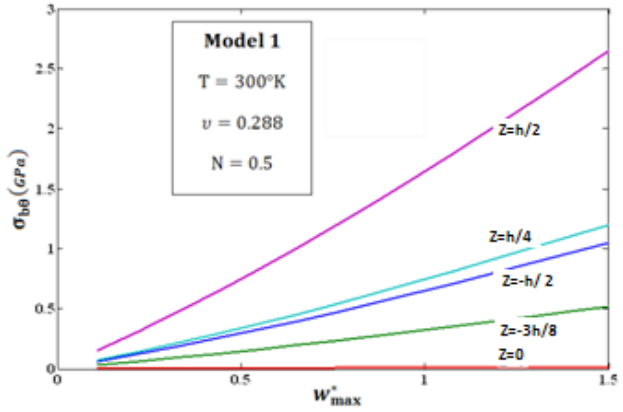

Fig. 12 Variation of circumferential stress with dimensionless maximum vibration amplitude on different surfaces for N = 0.5 at the inner edge

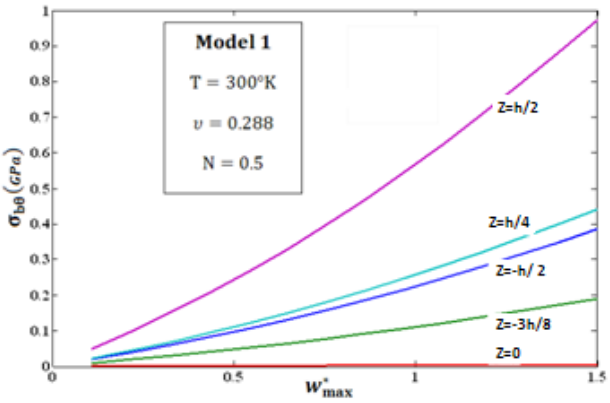

Fig. 13 Variation of circumferential stress with dimensionless maximum vibration amplitude on different surfaces for N = 0.5 at the outre edge

Fig. 14 demonstrates the variation of the radial bending stress at the inner edge of FG annular plate through the dimensionless thickness for N = 0.5. It shows that the radial stress is maximum on rich-ceramic surface $(z/h = 0.5)$and it is zero on neutral surface $(z/h = 0)$.

In Figs. 15 to 18 are plotted the variation of the bending stresses at the inner and outre edge of FG annular plate through the dimensionless thickness for different values of volume fraction index N.

From these figures, it is observed that that in the case of an isotropic material (plate made completely of metal and plate made completely of ceramic) the bending stresses distribution through the thickness of the plate at the clamped edges is linear and symmetric, but in the case of FG materials this distribution is non-linear, asymmetric and varies with (N) between the two lines representing the two linear cases which are confused with the two cases N = 0 (Ceramic) and N = ∞ (Metal).

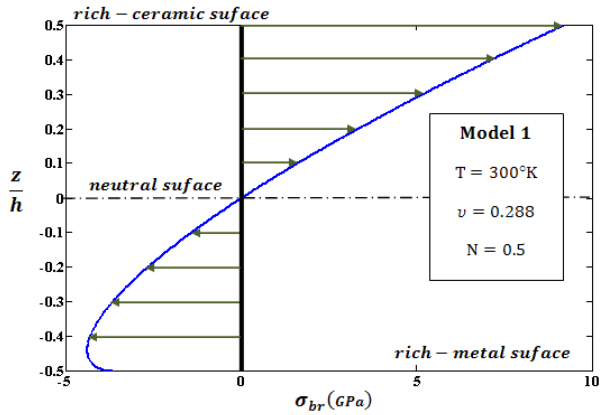

Fig. 14 Variation of the radial stress at the inner edge of FG annular plate through the dimensionless thickness for N = 0.5

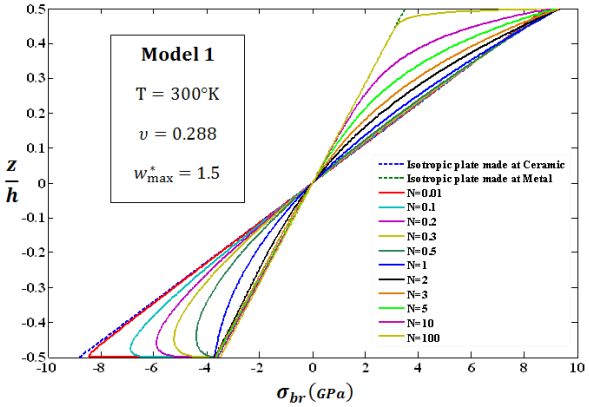

Fig. 15 Variation of the radial stress at the inner edge of FG annular plate through the dimensionless thickness for different values of volume fraction index N

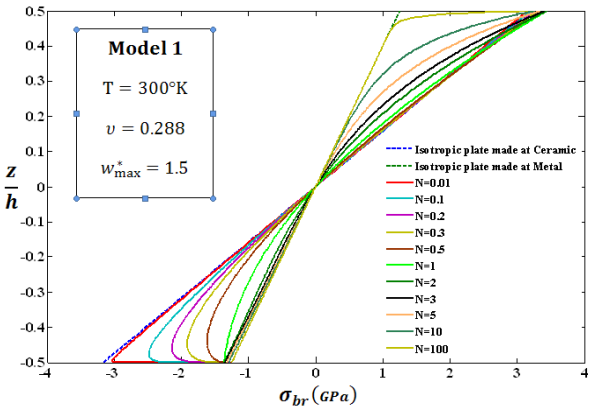

Fig. 16 Variation of the radial stress at the outre edge of FG annular plate through the dimensionless thickness for different values of volume fraction index N

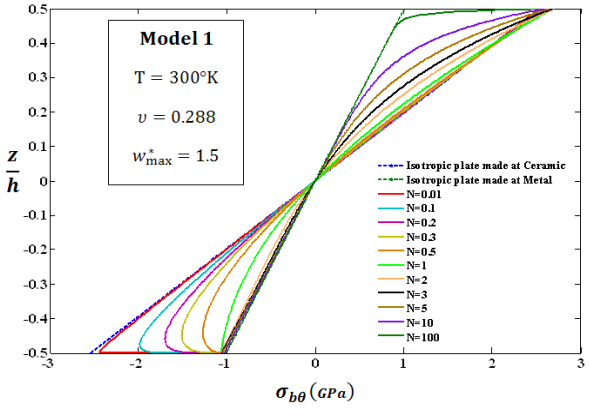

Fig. 17 Variation of the circumferential stress at the inner edge of FG annular plate through the dimensionless thickness for different values of volume fraction index N

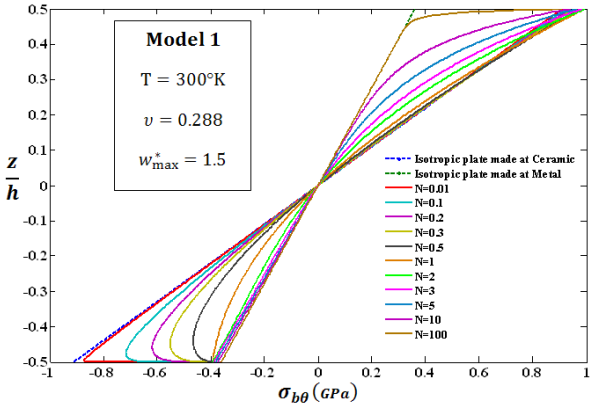

Fig. 18 Variation of the circumferential stress at the outre edge of FG annular plate through the dimensionless thickness for different values of volume fraction index N

VI. Conclusion

In order to investigate the effect of the volume fraction on the vibration behavior at large amplitude of a thin annular functionally graded plate, the theoretical model based on the classical plate theory and the Von Kármán geometrical non-linearity assumptions is used in this paper. For the low vibration amplitudes, the effect of volume fraction index on the frequencies is negligible, but he has considerable effect on the stresses in high vibration amplitudes.

References

[1] Amini, H., Rastgoo, A. and Soleimani, M., "Stress analysis for thick annular FGM plate", J. of Solid Mechanics, Vol. 4, (2009), 328-342.
[2] Li SR, Zhang JH, Zhao YG. Nonlinear thermomechanical post-buckling of circular FGM plate with geometric imperfection. Thin-Wall Struct (2007); 45:528–36.
[3] Allahverdizadeh, A., Naei, M.H. and Nikkhah Bahrami, M., "Nonlinear free and forced vibration analysis of thin circular functionally graded plates", Journal of Sound and Vibration, Vol. 310, (2007), 966–984.
[4] Chen, C.-S, "Nonlinear vibration of a shear deformable functionally graded plate", J. Compos. Struct., Vol. 68, (2005), 295–302.
[5] Reddy, J.N., Cheng, Z.Q., "Frequency of functionally graded plates with three-dimensional asymptotic approach", J. Eng. Mech., Vol. 129, (2003), 896–900.
[6] Ma LS, Wang TJ. Nonlinear bending and post-buckling of a functionally graded circular plate under mechanical and thermal loadings. Int J Solids Struct 2003; 40:3311–30
[7] L. Azrar, R. Benamar, R.G. White, A semi-analytical approach to the non-linear dynamic response problem of beams at large vibration amplitudes, part II: Multimode approach to the forced vibration analysis, Journal of Sound and Vibration 255 (2002) 1–41.
[8] S. A. Vera, M. Febbo, C. A. Rosit, A. E. Dolinko. 2002, Transverse vibrations of circular annular plates with edges elastically restrained against rotation, used in acoustic underwater transducers. Ocean Engineering 29,1201-1208
[9] Reddy JN, Wang CM, Kitipornchai S. Axisymmetric bending of functionally graded circular and annular plates. Eur J Mech A: Solids (1999); 18:185–99.
[10] L. Azrar, R. Benamar, R.G. White, A semi-analytical approach to the non-linear dynamic response. Problem of S–S and C–C beams at large vibration amplitudes. Part I: general theory and application to the single mode approach to free and forced vibration analysis, Journal of Sound and Vibration 224 (2) (1999) 377–395.
[11] Reddy JN, Praveen GN. Nonlinear transient thermoelastic analysis of functionally graded ceramic-metal plate. Int J Solids Struct (1998):35:4457–76.

[12] R. Benamar, M.M.K. Bennouna, R.G. White, The effects of large vibration amplitudes on the mode shapes and natural frequencies of thin elastic structures, part II: fully clamped rectangular isotropic plates, Journal of Sound and Vibration 164 (1991) 399–424.
[13] A. W. Leissa. Vibration of plates. 1969 Office of Technology Utilization. Washington.